Indian J Phys (May 2015) 89(5):445–452
DOI 10.1007/s12648-014-0601-8

ORIGINAL PAPER

Facile one step synthesis of novel TiO_2 nanocoral by sol–gel method using *Aloe vera* plant extract

K S Venkatesh[1], S R Krishnamoorthi[1], N S Palani[1], V Thirumal[1], S P Jose[2], F-M Wang[3] and R Ilangovan[1]*

[1]Nanoelectronics Laboratory, Department of Nanoscience and Technology, Alagappa University, Karaikudi 630 004, Tamil Nadu, India

[2]School of Physics, Madurai Kamaraj University, Madurai 625 021, Tamil Nadu, India

[3]Graduate Institute of Applied Science and Technology, National Taiwan University of Science and Technology, 43 Keelung Road, Section 4, Taipei 106, Taiwan

Received: 17 June 2014 / Accepted: 08 September 2014 / Published online: 12 October 2014

Abstract: Titanium oxide (TiO_2) nanoparticles (NPs) were synthesized by sol gel method using *Aloe vera* plant extract as a biological capping agent and a cauliflower-nanocoral morphology was observed in this technique. The assynthesized TiO_2 nanopowder was calcined at a range of temperatures (300–600 °C) for 1 h. The influence of *A. vera* plant extract on the thermal, structural and morphological properties of TiO_2 nanopowder was evaluated. Thermogravimetric analysis/differential thermal analysis was employed to study the thermal properties of the assynthesized TiO_2 nanopowder. The crystallinity, phase transformation and the crystallite size of the calcined samples were studied by X-ray diffraction technique. XRD result confirmed the presence of TiO_2 with anatase phase. FT Raman spectra showed the Raman active modes pertaining to the TiO_2 anatase phase and Raman band shift was also observed with respect to particle size variation. The different functional group vibrations of as dried pure *A. vera* plant extract were compared with the mixture of TiO_2 and *A. vera* plant extract by FT-IR analysis. The scanning electron microscopy images apparently showed the formation of spherical shaped NPs and also it demonstrated the effect of *A. vera* plant extract on the reduction of particles size. The surface area of the TiO_2 NPs was measured through Brunauer–Emmett–Teller analysis. Transmission electron microscopy images ascertained that the spherical shaped TiO_2 NPs were formed with cauliflower-nanocoral morphology decorated with nanopolyps with the size range between 15 and 30 nm.

Keywords: *Aloe vera*; TiO_2 nanocorals; X-ray diffraction; Raman spectroscopy; Electron microscopy

PACS Nos.: 81.16.Ta; 77.84.Bw; 61.05.cp; 78.30.Am; 78.30.Fs; 68.37.Hk; 68.37.Lp

1. Introduction

In the past few decades, nanomaterials are highly attracted by researchers to exploit their excellent properties for various applications. Among the semiconductor metal oxides, TiO_2 is a fascinating and one of the technologically important materials in the field of nanotechnology and it governs the keen interest of scientific community, due to its salient properties such as high chemical stability, wide band gap, good mechanical resistance and high optical transmittance in visible and IR spectral range [1]. TiO_2 exists in three polymorphs: rutile (Tetragonal), anatase (Tetragonal) and brookite (Orthorhombic). One dimensional TiO_2 nanowire structure has the potential application in dye sensitized solar cells (DSSCs) [2–6] and also TiO_2 is being greatly used in many applications such as photo catalysts [7, 8], gas sensors [9], electro chromic devices [10], antibacterial activity [11] and it also finds applications in biomedical sciences such as bone, tissue engineering and in pharmaceutical industries due to its non toxicity [12] and so on. TiO_2 nanoparticles (NPs) with different nanostructures have been synthesized by electrospinning method [13], hydrothermal method [14, 15], template method [16] etc.

Aloe barbadensis miller is one of the important medicinal plants and also it is known as the "Lily of the Desert". The raw pulp of *Aloe vera* contains approximately 0.5 % solid material consists of a variety of compounds including

*Corresponding author, E-mail: rajangamilangovan@gmail.com

water soluble and fat soluble vitamins, minerals, enzymes, polysaccharides, phenolic compounds, organic acids and remaining 99.5 % are water [17–19].

Synthesis of gold nano triangles and silver NPs using *A. vera* plant extract as reducing agent has been reported [20, 21]. Moreover, *A. vera* plant extract has been used to synthesize metal oxide NPs such as ZnO [22, 23], CuO [24], MFe_2O_4 (where M = Cu, Ni and Zn) NPs [25], hydroxyapatite (HAp) powders [26], In_2O_3 [27] and microorganisms have also been reported for the synthesis of metal oxides [28]. NPs synthesized by chemical methods are involved with toxic chemicals and adsorbed on its surface, which causes adverse effect in the medical applications. Synthesis of NPs using bio-capping agents offer non toxic, facile and one step synthesis with easiest protocol, sustainable and easy scale up to the industrial production at lower cost. Moreover, the uses of environmentally benign materials for the synthesis of NPs offer eco-friendliness and compatibility for pharmaceutical and biomedical applications as they do not use toxic chemical for the synthesis protocol [24]. Synthesis of different nanostructures is gaining a great importance in both fundamental scientific research and technological applications owing to their interesting physico-chemical properties. A nanocoral is one of the novel architecture and it has potential application in DSSCs. Synthesis of TiO_2 nanocorals is highly difficult and it has been achieved by means of multi step hydrothermal process [29], polymer gel templating procedure [30] etc. These methods involve multistep processes, time, power consuming, toxic chemicals and expensiveness and so on.

Sol–gel method is one of the best methods for the preparation of metal oxides. It offers an easy synthesis procedure to achieve nano scale counterparts by controlling the synthesis conditions. This method provides many advantages and to name a few are room temperature synthesis under atmospheric pressure, purity, homogeneity, to introduce desire amount of dopants, stoichiometry control and financially viable. However, it is very difficult to individually control the three reactions such as hydrolysis, condensation and agglomeration, which occurs simultaneously in sol–gel process. So, a slight change in experimental condition modifies the particle size and morphology [31, 32]. A fresh *A. vera* plant extract contains many biologically active components, such as polysaccharides vitamins, proteins, lipids, polyphenols, heterocyclic and carbonyl compounds and so on. In the extracellular synthesis of NPs using plants, on one hand, some biomolecules can act as reducing agent, on the other hand, some biological constituents can act as capping agent for the resulting NPs. As a result, the aggregation of resulting NPs could be impeded by means of stabilization due to the protein- nanoparticle interaction and also the surface morphology can be influenced by the shape-directing ability of the carbonyl compound present in the *A. vera* plant extract. Hence, it is anticipated that this synergistic effect of *A. vera* plant extract (both stabilization and capping) might influence on the morphology and size of TiO_2.

In this communication, the facile one step sol–gel synthesis of novel TiO_2 nanocoral architecture using *A. vera* plant extract as a bio-capping agent is reported. It has been clearly observed that *A. vera* plant extract proves its efficacy on the thermal, structural and morphological properties of TiO_2 NPs as expected. A novel TiO_2 nanocoral architecture through simple experimental procedure such as sol gel method using *A. vera* plant extract as bio-capping agent is demonstrated.

2. Experimental details

Titanium isopropoxide (SD Fine Chemicals), Ethanol, absolute (MERCK) and *A. vera* plant extract were used as starting materials for the preparation of pure and *A. vera* capped TiO_2 precursor solution. Fresh and matured leaves of *A. vera* plant were harvested from the local agricultural land. Then, 30 g of thoroughly washed *A. vera* leaves were finely cut and boiled in 100 ml of deionized water. The resulting extract was used for further experiments [20]. Pure TiO_2 precursor solution was prepared by drop wise addition of 3 ml of Titanium isopropoxide in 20 ml of ethanol under magnetic stirring. Similarly, *A. vera* capped TiO_2 precursor solution was prepared by adding 0.5, 0.75 and 1 ml of *A. vera* plant extract during the preparation of pure TiO_2 precursor solution and they were coded as 1AT, 2AT and 3AT respectively. After 3 h under continuous stirring, the pure and *A. vera* capped TiO_2 precursor solutions were subjected to heating (100 °C) under stirring, until the xerogel completely dried and finally cooled to room temperature. By adding titanium isopropoxide in ethanol solution, $Ti(OH)_4$ was formed. Upon subsequent heating at 100 °C, the formation of TiO_2 took place due to the condensation process. The relevant chemical reaction process were followed, as given in Eqs. (1a) and (1b).

$$\mathrm{Ti}\{\mathrm{OCH(CH_3)_2}\}_4 + 4\mathrm{C_2H_5OH} \longrightarrow \mathrm{Ti(OH)_4} + 4\mathrm{(CH_3)_2}\mathrm{-CH-O-C_2H_5} \quad (1a)$$

$$\mathrm{Ti(OH)_4} \xrightarrow{\Delta(100\ ^\circ\mathrm{C})} \mathrm{TiO_2} + 2\mathrm{H_2O} \quad (1b)$$

The dried precursor was crushed into fine powder using agate mortar and pestle. Finally, the grinded powder was calcined at different temperatures in a tubular furnace (Carbolite, UK) in an ambient atmosphere. Before calcination, the thermal behavior of the as-synthesized TiO_2 powder was analyzed by means of Thermo Gravimetric and Differential Thermal Analysis (EXSTAR

6000 TG/DTA) from ambient to 900 °C with the heating rate of 10 °C/min in air atmosphere. XRD pattern was recorded by Cu Kα radiation (1.54060 Å) using PANalytical X-PERT PRO diffractometer system. The morphology was examined by scanning electron microscopy (SEM) (Model: Hitachi S3000 H SEM). The surface area was measured by Brunauer–Emmett–Teller (BET) using MICROMETRICS ASAP 2020 POROSIMETER. FT- Raman spectra were obtained by BRUKER RFS 27 FT-Raman spectrometer. The functional group vibrations of the 2AT and the pure *A. vera* plant extract powders were analyzed by FTIR analysis (Model: Perkin Elmer Spectrum RX I). Transmission Electron Microscopy (Model: JEOL-200 FXII) was employed to confirm the nanocoral structure and also to measure the size of the NPs.

3. Results and discussion

In the preparation of TiO_2 precursor solution, it has been observed that the precursor solution is clear even after the addition of titanium isopropoxide with the ethanol solution, which manifests the complete dissolution of the metal alkoxide in the solvent. This clear solution immediately becomes to slurry with pale green colour followed by the addition of *A. vera* plant extract and it has been happened due to the rapid reaction of the precursor solution through hydrolysis and condensation caused by the presence of water molecules in *A. vera* plant extract. The colour change indicates the encapsulation of TiO_2 particles by small amount of solid biomolecules (0.5–1 %) contain in the *A. vera* plant extract and also the pale green colour becomes rich with respect to the increase of *A. vera* plant extract. The colour of the as-synthesized powder has been changed to pure white, after the calcination process which implies the elimination of biomolecules from the powder.

The TGA/DTA analysis has been performed for the as-synthesized (1AT and 3AT) TiO_2 nanopowder. In TGA curve of 1AT sample, the weight loss around 100 °C is attributed to the removal of physically and chemically entrapped water and a further weight loss at 210 °C is attributed to the elimination of organic matrix, as shown in Fig. 1(a). There is no further weight loss after 300 °C and in association with DTA curve, the oxidation process of the powder is initiated at the same temperature (300 °C), which indicates the formation of metal oxide. In the case of 3AT sample, physically and chemically entrapped water removed at 100 °C and the removal of organic matrix takes place around 235 °C, as shown in Fig. 1(b). This small increase in temperature for 3AT is due to the presence of more surface energy offered by the NPs compared to the 1AT sample. Hence it is understood that biological

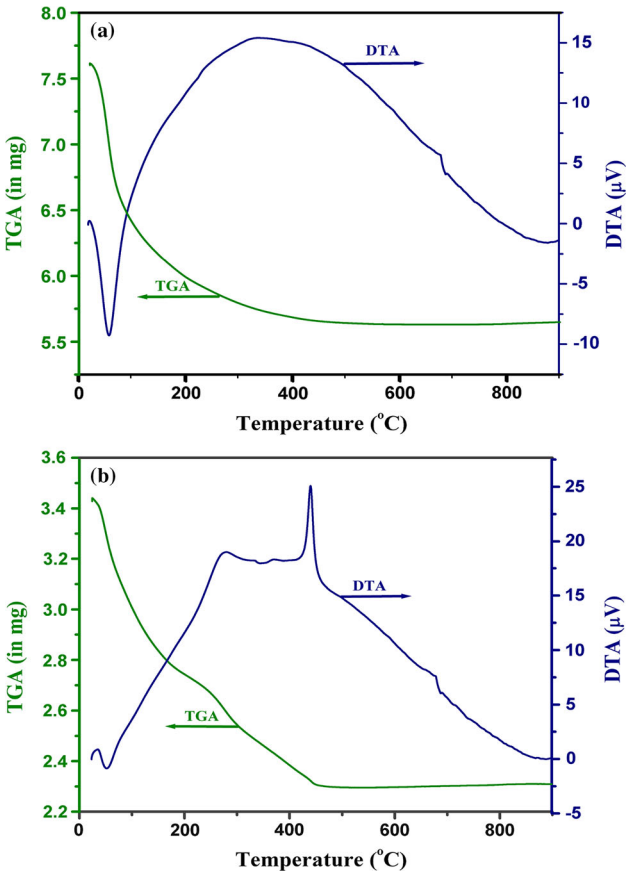

Fig. 1 TGA/DTA curve of as-synthesized TiO_2 nanopowder. (**a**) 1AT and (**b**) 3AT

molecules enter in the metal oxide matrix and serve as capping agent. In DTA curve (3AT) a small exothermic region around 300 °C indicates the crystallization of the TiO_2 nanopowder followed by the oxidation process. In TGA curve, the further weight loss is observed till 420 °C associated with the strong exothermic peak in DTA curve, which is due to complete removal of the sheath of biomass present over the NPs. In both cases, a small change observed at around 670 °C may be attributed to the phase transformation of TiO_2 from anatase to rutile.

As shown in the XRD pattern of 1AT and 2AT samples, the as-synthesized TiO_2 nanopowder is amorphous. After the calcination, the predominant peak found out for the 1AT, 2AT and 3AT samples at 25.3° (2θ) with (101) plane and other planes such as (004), (200), (211), (204), (116), (103), (112), (113), (105) are corresponding to anatase phase as shown in Fig. 2(a)–2(c). In the case of 1AT, the rutile phase of TiO_2 is also observed only at the calcination temperature of 600 °C and the planes (110), (101), (111), (210), (211), (220), (310) refers to the rutile phase, as shown in Fig. 2(a). All the observed diffraction peak values are closely match with the standard diffraction data (JCPDS File No: 89-4921, 89-4920). The crystallization

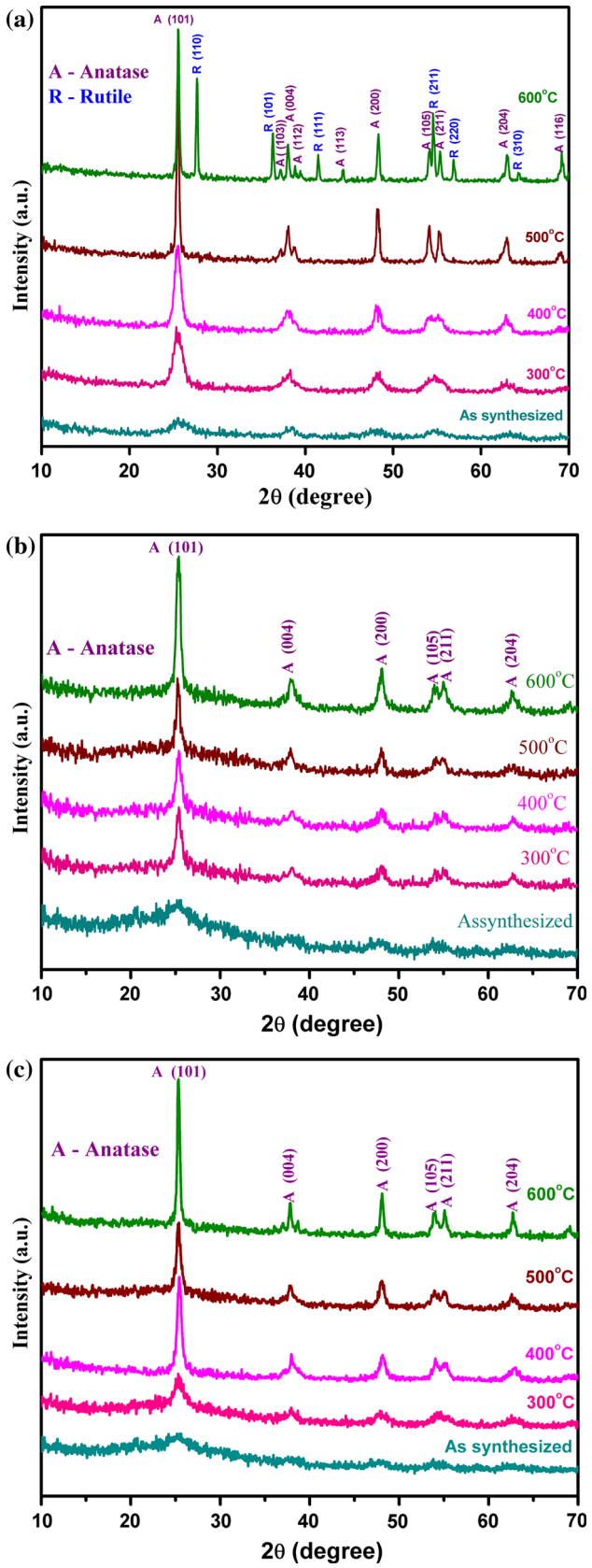

Fig. 2 XRD patterns of TiO_2 nanopowder. (**a**) 1AT, (**b**) 2AT and (**c**) 3AT

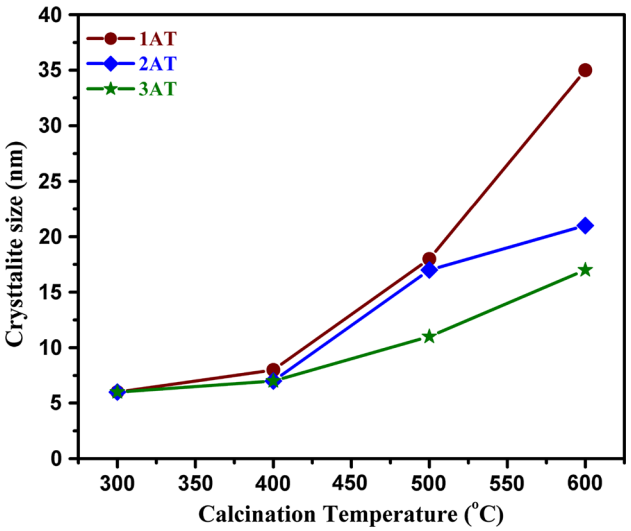

Fig. 3 Crystallite size versus calcination temperature of TiO_2 nanopowder

temperature of as-synthesized TiO_2 nanopowder has been observed at 300 °C for 1AT and 3AT samples and this is consistent with the TGA/DTA results. The free energy of rutile phase is always less than that of anatase phase, making the rutile is more stable phase at all temperatures. But the rutile phase has been not observed for 2AT and 3AT even at higher calcination temperature (600 °C) owing to higher concentration (0.75, 1 ml) of *A. vera* plant extract. The *A. vera* plant extract (0.75 onwards), which hinders the grain growth, thereby leads to the NPs and also retards the phase transformation. Hence, the phase transformation of TiO_2 from anatase to rutile can be controlled by bio-capping agent. Indeed, the improvement in the degree of crystallinity has been clearly observed with the increase of calcination temperature.

The crystallite size of the synthesized TiO_2 nanopowder has been calculated using scherrer equation (Eq. 2).

$$D = \frac{0.9\lambda}{\beta \cos\theta} \tag{2}$$

$$\frac{1}{d^2} = \frac{h^2 + k^2}{a^2} + \frac{l^2}{c} \tag{3}$$

where 0.9 is a constant, λ is the wavelength of X-ray source, β is the full width at the half maximum in radians, θ is the Bragg's diffraction angle. The effect of concentration of *A. vera* plant extract and the calcination temperature on the crystallite size of the synthesized TiO_2 nanopowder is presented in Fig. 3. The lattice constants are calculated using X ray diffraction data from the formula of Tetragonal crystal system (Eq. 3). The calculated lattice constants are presented in Table 1. These values are in close agreement with the standard values of both anatase and rutile phases

Table 1 Lattice constants of TiO_2 nanopowder

Sl. no.	Crystal system (tetragonal)	Standard values		Calculated values	
		a = b (Å)	c (Å)	a = b (Å)	c (Å)
1	Anatase	3.777	9.501	3.7856	9.5229
2	Rutile	4.584	2.953	4.5579	2.9524

Lattice constants of TiO_2 nanopowder

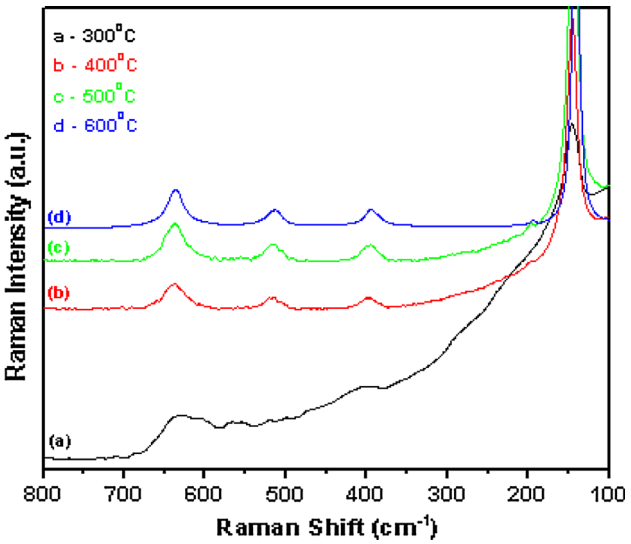

Fig. 4 FT Raman spectra of TiO_2 nanopowder (3AT)

of TiO_2. A small deviation in both phases of calculated lattice constant values with respect to those standard values may be due to the strain of the TiO_2 nanopowder caused by the heat treatment (calcination) and/or may be due to the instrumental error.

It is well known that TiO_2 exists in three polymorphs namely anatase, rutile and brookite. Rutile is thermodynamically stable, whereas anatase and brookite undergo irreversible exothermic transformation to rutile with respect to the range of temperature. Rutile, anatase and brookite phases of TiO_2 have 4, 6 and 36 Raman active modes, respectively [33, 34]. Figure 4(a)–4(c) show the FT- Raman spectra of TiO_2 nanopowder (3AT) calcined at 400 °C for 1 h. The appearance of strongest E_g mode at 144 cm^{-1} is due to the Ti–O streaching vibration bond which ascertains the presence of anatase phase in the TiO_2 nanopowder. The modes located at 144 (E_g), 197 cm^{-1} (E_g), 396.9 (B_{1g}), 515 (A_{1g}) and also 637 cm^{-1}(E_g) are responsible for the Raman active modes of anatase phase TiO_2 [35] and no other peaks have been detected, which indicates that the TiO_2 nanopowder posses anatase phase only. By comparing these spectra, it seems to be clear that the Raman bands are slightly shifted towards the higher wave number with respect to the increase of calcination

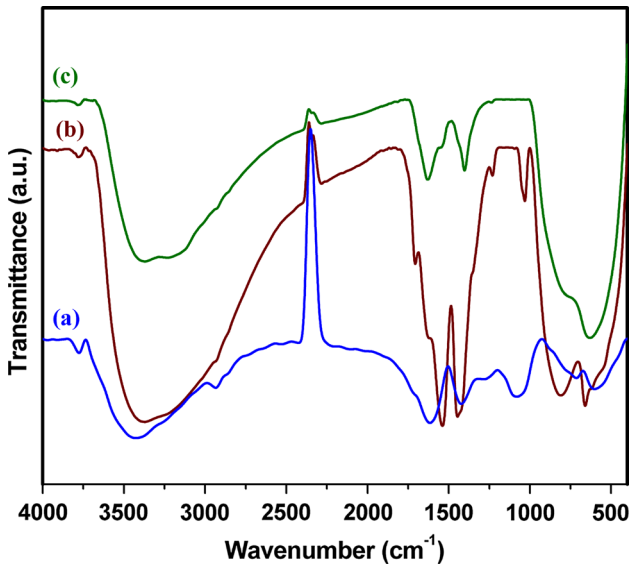

Fig. 5 FTIR spectra of *a* dried *Aloe vera* plant extract, *b* as synthesized TiO_2 nanopowder, *c* TiO_2 nanopowder calcined at 300 °C

temperature, which emphasizes the increase of the particle size. Also the increase of peak intensity with the increase of calcination temperature indicates the increase of crystallinity. There is no any Raman modes pertaining to the rutile phase and it suggested the absence of rutile phase and this result is consistent with the XRD results.

FTIR spectra of *A. vera* plant extract and TiO_2 nanoparticle are shown in Fig. 5(a)–5(c). A broad band at 3,423 cm^{-1} is assigned to hydrogen bonded –OH stretching vibration. A band observed at 1,615 cm^{-1} is attributed to the amide group vibration, which is a characteristic peak of proteins/enzymes [36]. The bands appeared at 1,421 and 1,080 are associated with carboxylic acid, C–N stretching vibration of amine group respectively, as shown in Fig. 5(a). This clearly indicates the presence of biomolecules and bio constituents of *A. vera* extract. A band shift occurs from 1,615 to 1,539 cm^{-1}, which indicates the binding of proteins with the surface of TiO_2 and thereby it leads to the stabilization of NPs. Furthermore, a band shifts from 1,421 to 1,442 and 1,080 to 1,034 cm^{-1} infer the contribution of carboxylic acid and amine groups respectively, which are the capping ligands for the encapsulation of TiO_2 NPs. There is a band shift from 3,423 to 3,372 cm^{-1}, which may be due to the condensation of Ti–OH group. A band at 659 cm^{-1} is attributed to the stretching vibration of TiO_2, as shown in Fig. 5(b). Finally, it can be noticed that the proteins/enzymes, carboxylic acid and amine groups present in the *A. vera* plant extract can lead to the formation of TiO_2 NPs through stabilization and encapsulation respectively [22]. Some of the bands appeared for as-synthesized sample have disappeared after the calcination, as shown in Fig. 5(c).

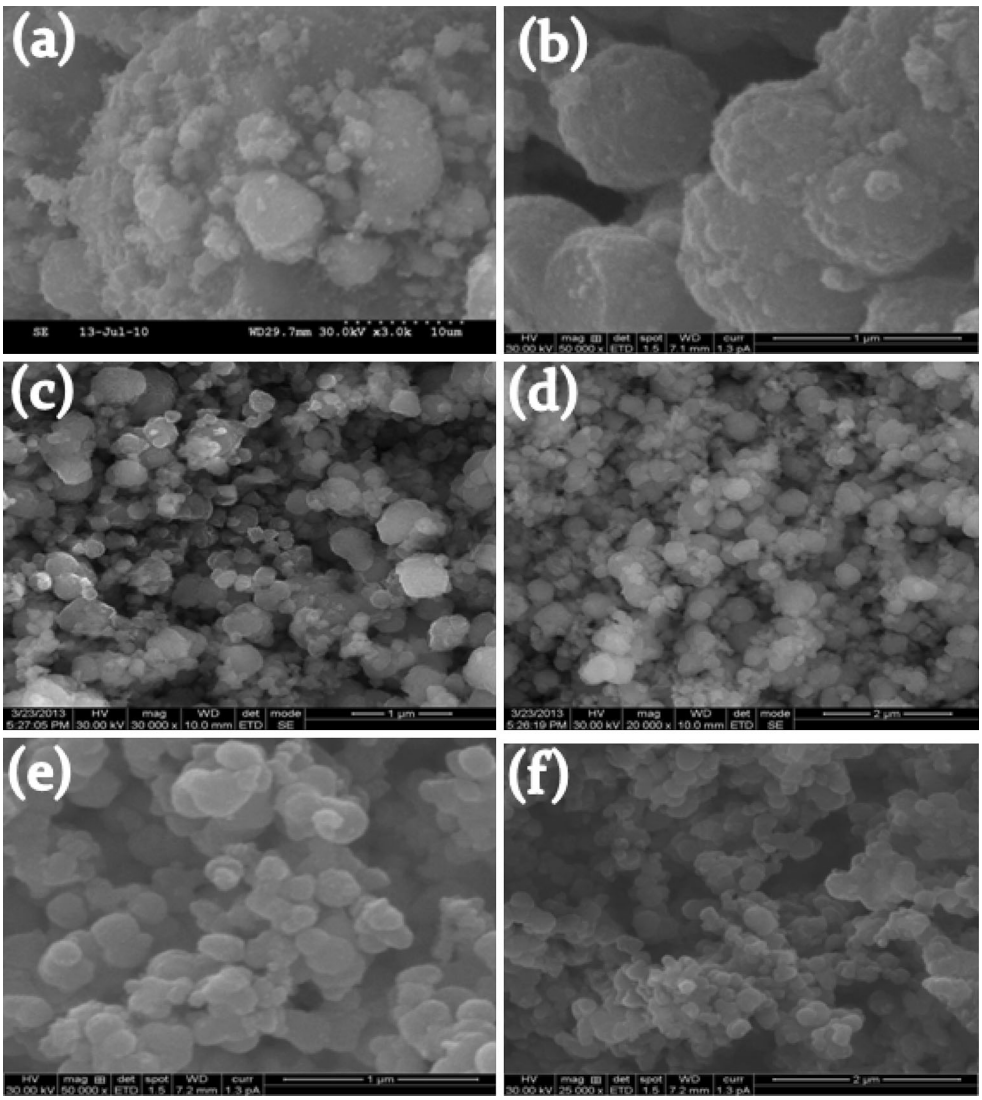

Fig. 6 SEM image of TiO_2 nanopowder calcined at 400 °C. (**a**) Pure TiO_2 without *Aloe vera* plant extract. (**b**) 1AT, (**c**) and (**d**) 2AT, (**e**) and (**f**) 3AT

Figure 6(a) shows the SEM image of pure TiO_2 powder, in which the particles are highly agglomerated due to the simultaneous hydrolysis, condensation and aggregation. It is apparently seen from the Fig. 6(b)–6(f) that the impact of *A. vera* plant extract is clearly observed on the control of agglomeration as well as reduction in particles size of TiO_2 nanopowder. It elucidates the decrease of particles size with the increase of *A. vera* plant extract and also it indicates the spherical shape of the particles. Moreover, the uniformity of the particles (2AT and 3AT) implies the well association of biomolecules with TiO_2 NPs during the synthesis process. In order to ascertain the morphology and particle size (3AT), it has been further subjected to TEM analysis.

The surface area of the TiO_2 nanocorals (3AT sample) calcined at 400 °C has been measured using nitrogen gas adsorption by BET analysis and the specific surface area is 27.6238 m^2/g.

As shown in the TEM image, it perspicuously depicted the presence of plausible nanocorals Fig. 7(a)–7(d) with the diameter in the range of 80–200 nm. It can be clearly visualize that the nanocorals are decorated with the nanopolyps of titanium oxide (TiO_2) having the size in the range between 15 and 30 nm. SAED pattens of the synthesized TiO_2 nanopowder show a polycrystalline nature in Fig. 7(e) and 7(f).

The possible growth mechanism for the resultant TiO_2 cauliflower morphology is still unclear but it is understood on the basis of observed experimental results presented in Fig. 8. As already discussed, the addition of *A. vera* extract results the change of TiO_2 precursor solution from its clear nature to slurry. This indicates the rapid reaction of *A. vera* extract with TiO_2 precursor solution. The growth mechanism may occur in two stages. Firstly, the protein/enzyme–nanoparticle interaction takes place i.e. the protein of the

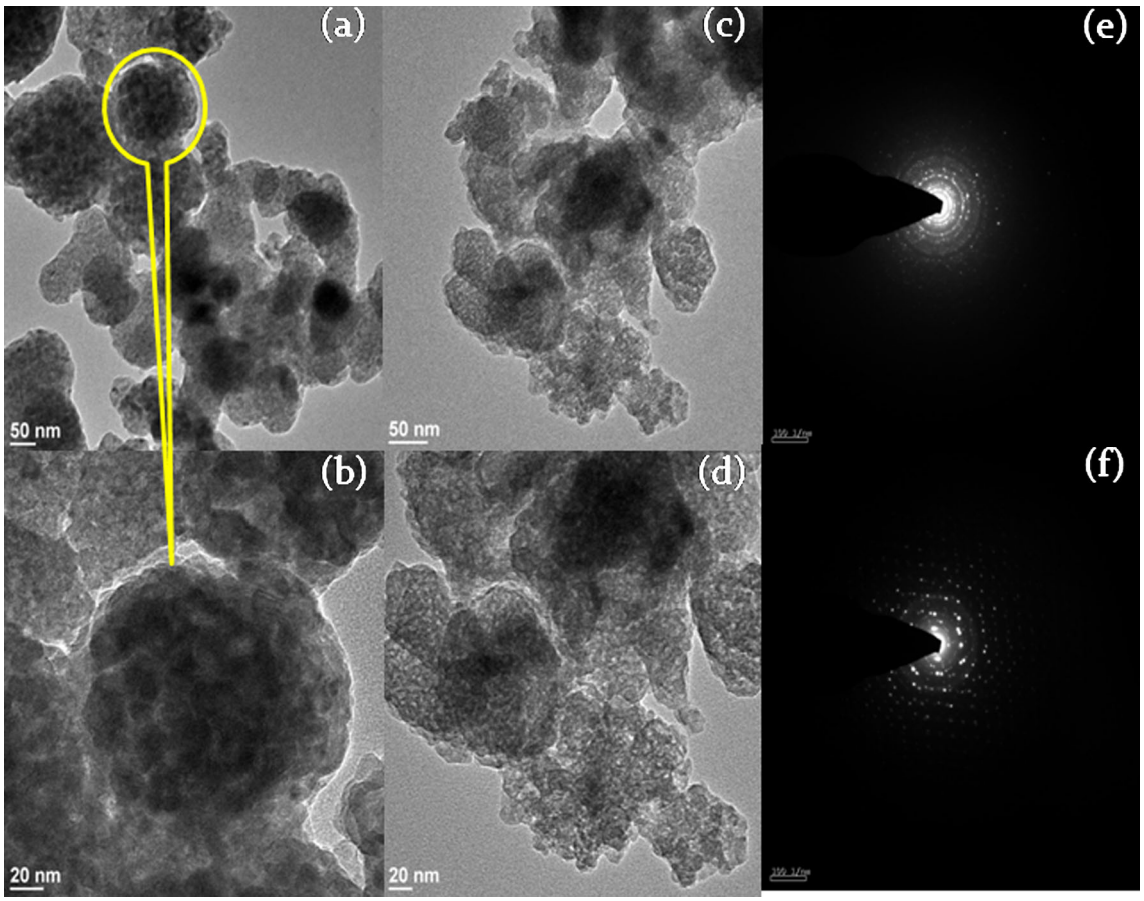

Fig. 7 TEM image of TiO_2 nanocorals calcined at 400 °C. (**a**), (**b**) 3AT, (**c**), (**d**) 1AT, (**e**), (**f**) SAED patterns of 3AT and 1AT

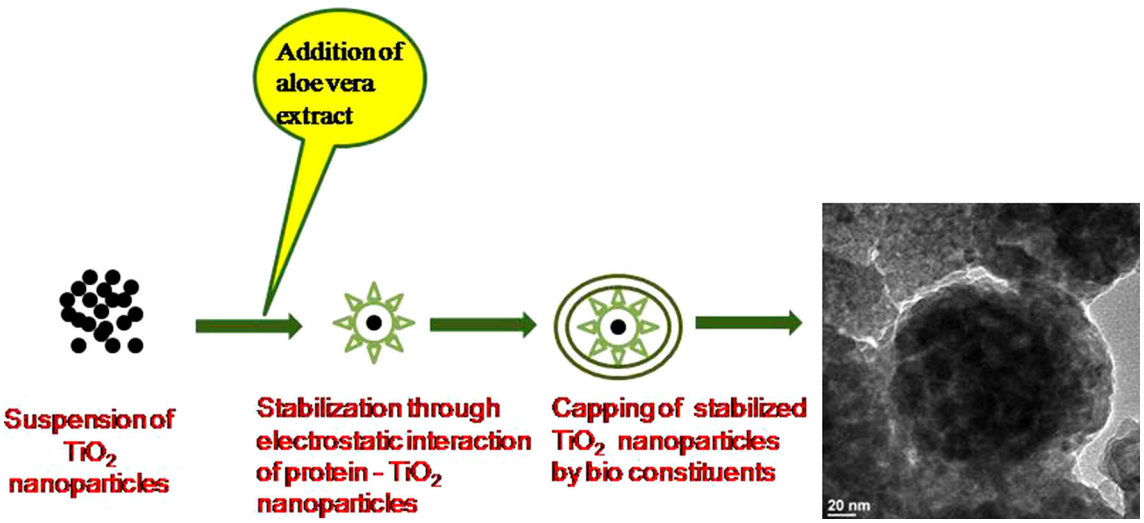

Fig. 8 Schematic illustration of the growth mechaniam of TiO_2 cauliflower-nanocoral morpholgy

A. vera extract can bind with the TiO_2 surface via electrostatic interaction. This is clearly supported by the band shift from 1,615 cm^{-1} to 1,539 cm^{-1} in the FTIR spectrum. In this stage, the aggregation of NPs could be effectively avoided and thus the stabilization of NPs is takes place by proteins, which is supposed to the formation of primary TiO_2 nanopolyps. Secondly, due to the shape-directing ability of carbonyl compounds and other such bio constituents of *A. vera* extract, the capping of TiO_2 nanopolyps stabilized by proteins takes place. During the

calcination at 400 °C, the removal of biological constituents also takes place and the spontaneous aggregation of primary TiO_2 nanopolyps results in the formation of cauliflower-nanocoral morphology. Hence, the formation of TiO_2 cauliflower-nanocoral morphology is due to the synergistic effect of *A. vera* extract.

4. Conclusions

A novel TiO_2 nanocoral architecture is obtained first time using *A. vera* plant extract as a bio-capping agent by sol–gel process. The concentration variation of *A. vera* plant extract enormously changes the particle size of TiO_2 nanopowder and thereby it leads to control the particle size. Thermal analysis reveals the crystallization temperature of 1AT and 3AT at 300 °C. The XRD analysis substantiates the presence of TiO_2 in anatase phase and also the rutile phase of TiO_2 nanopowder (1AT only) at 600 °C for the lower concentration (0.5 ml). Hence the phase transformation of TiO_2 nanoparticle depends on the concentration of *A. vera* plant extract. FT Raman spectra emphasize the presence of TiO_2 anatase phase (3AT) and the Raman band shifts with respect to the particle size variation. The biological molecules are responsible for the formation of TiO_2 NPs, which is analyzed by FTIR spectroscopy. The surface area is measured by BET analysis and it is found to be 27.6238 m^2/g. SEM images depict the homogeneity, formation of TiO_2 NPs with spherical shape and also the reduction of particle size with respect to the concentration of *A. vera* plant extract. Furthermore, TEM images demonstrate the plausible nanocorals decorated with the nanopolyps having the diameter in the range of 15–30 nm.

Acknowledgments The work was financially assisted by University Grants Commission through the scheme of UGC Major Research Project [No. F. 40-74/2011 (SR)] and highly acknowledged. Also, the authors thank School of Physics, Alagappa University, Karaikudi for extending XRD facility and DST PURSE funded HRSEM instrumental facility extended by Department of Industrial Chemistry, Alagappa university, Karaikudi and Indian Institute of Technology (IIT Madras—SAIF) Chennai for extending the FT Raman instrument facility.

References

[1] D R Lide *Handbook of Chemistry and Physics* 71st edn. (Boca Raton: F1 CRC) (1991)
[2] W Q Wu, Y F Xu, C Y Su and DB Kuang *Energy Environ. Sci.* **7** 644 (2014)
[3] W Q Wu, Y F Xu, H S Rao, H L Feng, C Y Su and DB Kuang *Angew. Chem.* **19** 4816 (2014)
[4] W Q Wu, B X Lei, H S Rao, Y F Xu, Y F Wang, C Y Su and D B Kuang *Sci. Rep.* **3** 1352 (2013)
[5] J N Hart, D Menzies, Y B Cheng, G P Simon and L Spiccia *J Sol–Gel Sci. Technol.* **40** 45 (2006)
[6] B Oregan and M A Gratzel *Nature* **353** 737 (1991)
[7] S Sarmah and A Kumar *Indian J. Phys.* **85** 713 (2011)
[8] A Fujishima and K Honda *Nature* **238** 37 (1972)
[9] M R Vaezi, S Khoby Shendy and T Ebadzadeh *Indian J. Phys.* **86** 9 (2012)
[10] S Berger, A Ghicov, Y C Nah and P Schmuki *Langmuir* **25** 4841 (2009)
[11] G Fu, P S Vary and C T Lin *J. Phys. Chem. B* **109** 8889 (2005)
[12] L C Gerhardt, G M R Jell and A R Boccaccini *J. Mater. Sci. Mater. M* **18** 1287 (2007)
[13] H Y Chen, T L Zhang, J Fan, D B Kuang and C Y Su *Appl. Mater. Interfaces.* **5** 9205 (2013)
[14] G Guo, B Yu, P Yu and X Chen *Talanta* **79** 570 (2009)
[15] J Y Liao, B X Lei, H Y Chen, D B Kuang and C Y Su *Energy Environ. Sci.* **5** 5750 (2012)
[16] Z Wang, B Huang, Y Dai, X Zhang, X Qin, Z Li, Z Zheng, H Cheng and L Guo *Cryst. Eng. Comm.* **14** 4578 (2012)
[17] K Eshun and Q He *Crit. Rev. Food Sci. Nutr.* **44** 91 (2004)
[18] M D Boudreau and F A Beland *J. Environ. Sci. Health C* **24** 103 (2006)
[19] J H Hamman *Molecules* **13** 1599 (2008)
[20] S P Chandran, M Chandhary, R Pasricha, A Ahmad and M Sastry *Biotechnol. Prog.* **22** 577 (2006)
[21] Y Zhang, D Yang, Y Kong, X Wang, O Pandoli and G Gao *Nano Biomed. Eng.* **2** 252 (2010)
[22] G Sangeetha, S Rajeshwari and R Venckatesh *Mater. Res. Bullet.* **46** 2560 (2011)
[23] G Sangeetha, S Rajeshwari and R Venckatesh *Prog. Nat. Sci.* **22** 693 (2012)
[24] G Sangeetha, S Rajeshwari and R Venckatesh *Spectrochim. Acta A* **97** 1140 (2012)
[25] P Laokul, V Amornkitbamrung, S Seraphin and S Maensiri *Curr. Appl. Phys.* **11** 101 (2011)
[26] J Klinkaewnarong, E Swatsitang, C Masingboon, S Seraphin and S Maensiri *Curr. Appl. Phys.* **10** 521 (2010)
[27] S Maensiri, P Laokul, J Klinkaewnarong, S Phokha, V Promarak and S Seraphin *J Optoelectron. Adv. Mater.* **10** 161 (2008)
[28] K S Venkatesh, N S Palani, S R Krishnamoorthi, V Thirumal and R Ilangovan *AIP Conf. Proc.* **1536** 93 (2013)
[29] S S Mali, C A Betty, P N Bhosale and P S Patil *Electrochim. Acta* **59** 113 (2012)
[30] R A Caruso, M Giersig, F Willig and M Antonietti *Langmuir* **14** 6333 (1998)
[31] A Golubovic, M Scepanovic, A Kremenovic, S Askrabic, V Berec, Z Dohcevic-Mitrovic and Z V Popovic *J. Sol Gel Sci. Technol.* **49** 311 (2009)
[32] M Niederberger *Acc. Chem. Res.* **40** 793 (2007)
[33] K Porkodi and S D Arokiasamy *Mater. Charact.* **58** 495 (2007)
[34] T Ohsaka, F Izumi and Y Fujiki *J. Raman Spectrosc.* **7** 321 (1978)
[35] M Hudlikar, S Joglekar, M Dhaygude and K Kodam *Mater. Lett.* **75** 196 (2012)
[36] S S Shankar, A Ahmad and M Sastry *Biotechnol. Prog.* **19** 1627 (2003)